FTM2003-01, Version 1.1, May 14, 2003

DISPIs and/or Filters for AMEX

Rob P. Olling[1,2]
[1]US Naval Observatory, [2]USRA

ABSTRACT

This memo reviews some of the trades regarding a grating and a set of filters for the AMEX mission.

1. Introduction

To date, virtually nothing is known about the vast majority of stars: physical parameters derived from high-resolution spectra are available for 3,356 stars (Cayrel de Strobel, Soubrian & Ralite 2001), uvby-β data exists for about 63,000 stars (Hauck & Mermilliod 1998), two-dimensional spectral classification (spectral type and luminosity class) exists for about 160,000 stars (Houk and collaborators 1971–2000), BV photometry is available for about two million stars brighter than $V \sim 11$ in the Tycho-2 catalog (Høg *et al.* 2000), while JHK photometry exists for 470 million stars brtighter than $K \sim 14.3$ ($V \lesssim 18$) in the 2MASS data products (Cutri *et al.* 2003). Low-accuracy photographic photometry (0.3 mag) is available for about 10^9 stars on the sky survey plates down to $V \sim 21$ (Monet *et al.*, UNSO-B 2003)

In the simplest form, spectral classification comprises of the determination of the stellar "color," where color could be any combination of UV/optical/NIR magnitudes. To first order, stellar spectra follow the black-body distribution, so that the observed color can be directly related to the effective temperature (T_{eff}) of the star under investigation. That is to say, for a black-body spectrum, the "shape of the continuum spectrum," and hence the stellar color is uniquely related to T_{eff}. Fortunately for astrophysicists, the spectra of stars deviate from the black-body law so that other properties besides T_{eff} can be inferred. The aim of spectral classification is to infer as many *physical* properties as possible from the obtained spectra.

1.1. Spectral Classification

One- and two-dimensional stellar classification based on intermediate-resolution (objective-prism) spectra goes some way towards this goal because the spectral type (and luminosity class) are

determined from line-ratios rather than the shape of the stellar continuum. This has the advantage that the spectral type (roughly proportional to T_{eff}) is determined independently from the often large amount of interstellar extinction. The intrinsic luminosity (M_V) can be approximated from the luminosity class (2D classification). In combination with broad-band colors one can thus obtain rough determinations of T_{eff}, extinction-corrected apparent magnitude (V_0), absolute magnitude (M_V), and interstellar extinction (A_V). The most extensive work in this field has been performed by Nancy Houk and collaborators in her effort to classify all stars in the Henry Draper catalog. This work is done by visual inspection of objective-prism plate material with a resolution of about 10 Å (0.2 Å at Hγ). Recently, in a pilot study Bailer-Jones and collaborators (Bailer-Jones, Irwin, & von Hippel 1998) have analyzed a digitized version of some of the Michigan plates employing artificial neural network (ANN) methods. The successful application of the ANN method to real data inspired Bailer-Jones and collaborators to further develop this method and generalize it by application to spectra obtained from model atmospheres (Bailer-Jones 2000, 2002; Willemsen, Bailer-Jones, Kaempf, & de Boer 2003). Also note that the baseline for the GAIA (DIVA) mission is (was) to employ ANN techniques to classify their photometric data.

High-resolution spectroscopy has yielded the most precise determinations of physical parameters. Currently, high-resolutionn spectroscopy is routinely used to determine T_{eff}, surface gravity [$log(g)$], metallicity ([Fe/H]), α-element enhancement ([α/Fe]), Lithium abundance ([Li/H]), and various "metallicity peculiarities." However, the results depend on the particular methods eployed to derive the quantities. For example, Soubrian, Katz & Cayrel (1998) compared parameters as determined from high-resolution spectra of Sun-like stars, and find an RMS difference among the reported values for $log(g)$, T_{eff} and [Fe/H] of 0.25 dex, 2% and 0.1 dex, respectively. Thus, the systematic errors associated with each method dominate the final achievable accuracy, at this moment in time. The internal errors for these methods of parameter estimation are substantially smaller.

1.2. Continuum-based Methods

Alternatively, one can also employ the shape of the emission at much lower resolution to determine the astrophysical parameters. Several narrow-band filter systems (e.g., uvby-β) have been devised to do just that. The location and widths of these bands have been chosen to coincide with spectral features that are sensitive to the to-be-determined parameters. The results obtained for such systems are calibrated against (one or more) high-res spectroscopic studies. Recent developments indicate that the bands are not required to be narrow: spectral classification is also possible with broader bands provided that the signal-to-noise ratio is sufficiently large. In fact, Olling's results for a 7-filter intermediate band system (FTM2001-03, FTM2001-07, FTM2001-15) indicate

that the precision with which $log(g)$ can be determined to:

$$\Delta log(g) \approx 0.0367 \times \left(\sqrt{1+15.5\Delta V_7}-1\right) \pm 0.05 \quad (1)$$

$$\Delta log(g) \approx 0.0367 \times \left(\sqrt{1+38,777 \times log(1+\frac{1}{SNR_7})}-1\right) \quad (2)$$

$$\Delta V_7 \approx \Delta log(g) \times [\,3.51+47.7\Delta log(g)\,] \quad (3)$$

where ΔV_7 (in milli-magnitudes) is the average error per band, for a 7-band filter set. Thus, for such a system, errors of 0.125, 0.25 and 0.5 dex in $log(g)$ can be achieved for $\Delta V \sim 1.2$, 3.9, and 14 mmag, respectively (and/or signal-to-noise ratios of SNR_7=916, 281, and 79, respectively). I present the dependence of the classification error on magnitude errors in figure 1. In this figure, classification results for $\Delta log(g)$ are presented for three different "filter sets:" 1) Olling's (2001) 7-band system, 2) Willemsen and collaborators' (2003) DISPI analysis, and 3) Bailer-Jones' (2000) analysis of simulated low-resolution ($\lambda/\Delta\lambda = 17.5$) long-slit spectra. Before plotting, all systems were brought onto the same sensitivity scale by calculating the equivalent photometric error (and/or SNR) in a 7-band system[1].

2. SNR Calculations for the "DIVA DISPIs"

The results derived in Willemsen *et al.*(2003; hereafter WEA2003) paper are based on an assumed readnoise level of 2 electrons per read. Furthermore, it was assumed that an on-chip 4x binning in the cross-scan direction can be achieved. With this set of assumptions, it was shown that good stellar classification can be achieved, even in the absence of the data from the UV telescope.

In this memo, I will estimate how this classification performance changes as a function of various parameters not considered by WEA2003, such as 1) increased nosie level, 2) different cross-scan binning

Table 1

V	SNR per_band dV	dTeff	dlog(g)	d[Fe/H]	dA_V
mag	mmag	[%]	[dex]	[dex]	[mag]

[1]Sensitivity scaling is accomplished by determining the number of photo-electrons (assuming photon statistics) that correspond to a given photometric error in mmag, or a SNR. This number of electrons is then multipled by the number of bands in the system, and divided by the number of bands in the reference system (i.e., 7). The equivalent photometric error (and/or SNR) is then determined, again using photon statistics.

9.0	1236	0.8		~0.1		
12.0	292	3.4	1- 6	0.20-0.60	0.1 -0.25	0.05-0.15
13.5	126	8.0	2- 8	0.25-0.90	0.2 -0.50	0.07-0.20
15.0	44	23.0	3-15	0.50-1.25	0.25-1.25	0.22-0.40

This classification performance is significantly better than anything available right now for such faint stars. Also note that any of the individual colors [e.g., $(c_1 - c_2), (c_1 - c_3), ...(c_1 - c_{10})$, etc.] will be determined about three times better[2] than the accuracy achieved for T_{eff}.

The results depend strongly upon apparent magnitude (s/N ratio). Note that the poor T_{eff} and $log(g)$ results will improve significantly when accurate UV data is available. Thus, a re-evaluation of the grating parameters might be in place so as to "move the grating response to the blue." [3]

Note that for classification purposes, a high spectral resolution is not required. In fact, a multi-band system with just 7–15 bands will perform rather well, provided that the signal-to-noise ratio exceeds 100 per band (e.g., Bailer-Jones (2000); Olling, (FTM2001-03), (FTM2001-07), (FTM2001-15); see http://ad.usno.navy.mil/∼olling/FAME/rpo_fame.htm). Thus, most likely, the high resolution of the DIVA grating is overkill. We will exploit this property later on. In fact, for the purpose of showing the utility of the DISPIs for the classification of stars and the determination of extinction, it is sufficient to show how the SNR scales for the case of a simulated resolution of $R_\lambda = 10$.

Thus, this document is organized as follows. In the table above, I have indicated the signal-to-noise ratios at magnitudes 12, 13.5 and 15 for WEA2003's assumptions for the performance of the CCDs. So as to achieve the classification accuracy better or equal to the WEA2003 values, the SNR of any other nosie model needs to exceed the values tabulated in Table 1. Thus, the benchmark SNR values are: 292, 126, 44 for excellent, good and acceptable results.

In the remainder of thei memo, I develop several noise models and compare the resulting SNR values: between ther grating & filters case, and with the WEA2003 values. We can live with a noise model if the SNR exceeds 45 per band, and we're happy if we can boost it too ≥ 200 or so.

---

[2]For the SNR calculation, I assume that the optical waveband is divided in 10 bands of equal width ($R \equiv \lambda/\Delta\lambda \sim 10$), that the number of electrons in the astrometric band equals 214,000 for a V=9 A0V star, and that the grating efficiency of ϵ_G=60%. Thus, the total number of electrons per band is assumed to equal 12,840 at V=9. The actual SNR is determined from the relation below.

[3]From the QE and grating response curves in WEA2003 (their figure 2) it appears that a wavelength scale $\frac{3}{4}$ times smaller would accommodate just that, if the grating's efficiency does not decrease below the design value of 60%. I do not know whether this is possible.

3. The Grating Case

To approximate the expected SNR values, I assume a "flat spectrum" source, i.e., all wavelength produce the same number of photo-electrons. Furthermore, I assume that the DISPI (dispersed image) has a length L_λ of 180 physical pixels in the cross-scan/dispersion direction and a width W_X of 6 pixels in the in-scan direction, and that the in-scan and cross-scan distribution functions are pillboxes. In this model, the DISPI comprises 180x6=1,080 pixels, each with 11.9 electrons at V=9. Thus, the signal per pixel is a function of magnitude: $S^G_{e/p}(V) = 11.9 \times 2.512^{9-V}$ electrons. For an effective grating resolution R_G of 10, the number of physical cross-scan pixels per wavelength-resolution-element is huge: $18 \times (10/R_G)$. Given that 10 bands suffices for classsification purposes, the spectral over-sampling suggests that the grating can be run in a lower resolution mode.

Thus, each effective waveband will contain a total of $N^G_{pix,S} = L_\lambda/R_G \times W_X = 1,080/R_G$ pixels that contribute to both the sinal and noise levels. Now, the signal-level per pixel per waveband equals $Signal^{G,1} = 12,840/R_G$ photo electrons (see also footnote 1). The noise calculation depends on the readnoise level *per read* (E_R), the achievable on-chip binning in the cross-scan direction (BX) and the sky background (E_S). Thus, the total number of pixels that contribute to the *read*noise equals $N^G_{pix,R} = L_\lambda/R_G/BX \times W_X = N^G_{pix,S}/BX$, while the number of "*sky*pixels" is equal to the number of source pixels, Furthermore, each star is observed N^G_{obs} times. With these considerations, the signal per observation, the total signal, the noise and SNR levels are given by:

$$
\begin{aligned}
Signal^{G,1} &= \frac{S^G_{e/p}(V)}{R_G} \times (L_\lambda \times W_X) && (4)\\
Signal^{G} &= Signal^{G,1} \times N^G_{obs} && (5)\\
(Noise^G)^2 &= Signal^G + N_{obs} \times (N_{pix,R} \times E_R^2 + N_{pix,S} \times E_S^2) \\
&= Signal^G \left(1 + \frac{E_R^2/BX + E_S^2}{S^G_{e/p}(V)}\right) && (6)\\
SNR^G &= \frac{Signal^G}{Noise^G} \\
&= \sqrt{Signal^{G,1} \times N^G_{obs}} \; / \; \sqrt{1 + \frac{E_R^2/BX + E_S^2}{S^G_{e/p}(V)}} && (7)
\end{aligned}
$$

Thus, in case the signal level per pixel substantially exceeds the variance of the noise, the denominator is approximately unity and the SNR increases as the square-root of the number of observations. For the WEA2003 case, with $E_R = 2, BX = 4, E_S = 0.04$ and $S^G_{e/p}(9) = 11.9$, this is indeed the case (denominator=1.04).

4. The Filter Case

The SNR calculations change for the case of a set of R_F filters. R_F should be larger than six so as to be able to solve for the astrophysical parameters and extinction. Below, I scale the results to $R_F = 7$

First of all, the grating loss of $(1 - \epsilon_G)$ is not incurred, so that the number of photo electrons per band per observation increases by a factor $1/\epsilon_G$. Also, the signal level changes as the inverse of the change in bandwidth, by a factor R_G/R_F. For surface-brightness considerations,the number of cross-scan pixels is reduced in this non-dispersive case to $2W_X$ so that[4] the signal level per pixel is increased by a factor $(L_\lambda/R_G)/(2W_X) = 1.5$ with respect to the grating case. On the down-side, the number of observations is reduced by the number of filters to $N^F_{obs} = N^G_{obs}/R_F$ because only one filter rather than the whole spectrum can be observed per CCD crossing. With these considerations, the signal per observation, the total signal, the signal per observation per pixel, and the SNR are given by:

$$Signal^{F,1} = \frac{Signal^{G,1}}{\epsilon_G}\left(\frac{R_G}{R_F}\right) \tag{8}$$

$$\begin{aligned} Signal^F &= Signal^{F,1} \times N^F_{obs} = Signal^{F,1} \times N^G_{obs}/R_F \\ &= \frac{R_G}{\epsilon_G R_F^2} \times Signal^G \approx 0.34\left(\frac{R_G}{10}\right)\left(\frac{0.6}{\epsilon_G}\right)\left(\frac{7}{R_F}\right)^2 \times Signal^G \end{aligned} \tag{9}$$

$$\begin{aligned} S^F_{e/p}(V) &= \frac{Signal^{F,1}}{W_X \times 2W_X} = \frac{R_G/R_F\ Signal^{S,1}}{2\epsilon_G W_X^2} = \frac{R_G/R_F}{2\epsilon_G W_X^2}\left(\frac{S^G_{e/p}(V)}{R_G}\right)(L_\lambda W_X) \end{aligned} \tag{10}$$

$$= S^G_{e/p}(V) \times \frac{L_\lambda}{\epsilon_G R_F \times 2W_X} = 3.57\left(\frac{L_\lambda}{180}\right)\left(\frac{7}{R_F}\right)\left(\frac{0.6}{\epsilon_G}\right) S^G_{e/p}(V) \tag{11}$$

$$(Noise^F)^2 = Signal^F\left(1 + \frac{E_R^2/BX + E_S^2}{S^F_{e/p}(V)}\right) \tag{12}$$

$$SNR^F = \frac{Signal^F}{Noise^F} = \sqrt{Signal^{F,1} \times N^F_{obs}}\ /\ \sqrt{1 + \frac{E_R^2/BX + E_S^2}{S^F_{e/p}(V)}} \tag{13}$$

$$= \sqrt{\frac{R_G}{\epsilon_G R_F^2}}\sqrt{Signal^S}\ /\ \sqrt{1 + \frac{2\epsilon_G R_F W_X}{L_\lambda}\left(\frac{E_R^2/BX + E_S^2}{S^S_{e/p}(V)}\right)} \tag{14}$$

[4]The mirror dimension in cross-scan direction is 50% of in-scan direction

5. Grating versus Filters

I define the grating-filters efficiency $E_{G/F}$ to equal $(Signal^G/Signal^F)^2$. Thus, $E_{G/F}$ is indicative of the ratio of the required observing time to reach a given SNR:

$$E_{G/F} \equiv \left(\frac{SNR^G}{SNR^F}\right)^2 = \left(\frac{\epsilon_G R_F^2}{R_G}\right) \times \left(\frac{1+\frac{E_R^2/BX+E_S^2}{3.57 S^G_{e/p}(V)\left(\frac{L_\lambda}{180}\frac{7}{R_F}\right)\left(\frac{0.6}{\epsilon_G}\right)}}{1+\frac{E_R^2/BX+E_S^2}{S^G_{e/p}(V)}}\right) \quad (15)$$

In the high and low SNR regimes, eqn. (15) simplifies to:

$$E_{G/F}(SNR\uparrow) \approx \frac{\epsilon_G R_F^2}{R_G} \approx 2.9\left(\frac{\epsilon_G}{0.6}\right)\left(\frac{R_F}{7}\right)^2\left(\frac{10}{R_G}\right) \quad (16)$$

$$E_{G/F}(SNR\downarrow) \approx \left(\frac{\epsilon_G R_F^2}{R_G}\right)\left(\frac{2\epsilon_G R_F W_X}{L_\lambda}\right) = \left(\frac{2\epsilon_G^2 R_F^3 W_X}{R_G L_\lambda}\right) \quad (17)$$

$$\approx 0.82\left(\frac{\epsilon_G}{0.6}\right)^2\left(\frac{R_F}{7}\right)^3\left(\frac{10}{R_G}\right)\left(\frac{180}{L_\lambda}\right) \quad (18)$$

Equation (16) shows that for typical resolutions, the grating solution is almost always preferred in the high SNR regime, unless the grating efficiency is very low, or a small number of filters is chosen, or a large number of "grating-bands" are used. Thus, we need to control the grating efficiency for the AMEX mission. A mission with too few filters or too large R_G are not useful, because of the limited astrophysical returns, and a too-high resolution, respectively.

In the low SNR regime, we see that for the given set of parameters, a 7-filter set would outperform the grating. However, there are two "easy" fixes to this problem. A) Make the grating more efficient: $\epsilon_G = 0.66$ would do. B) Decrease the length of the DISPIs to $L_\lambda \lesssim 148$. As mentioned above, for a resolution of R_G of 10, the DISPIs have 18 pixels per resolution element. Thus a dispersion that is a factor of two or three smaller would still yield sufficient sampling of the "spectrum." Finally, one can make equation (16) independent of noise level by setting the pre-factor in equation 11 equal to unity: that is to say, $1 \equiv 3.57\left(\frac{L_\lambda}{180}\right)\left(\frac{7}{R_F}\right)\left(\frac{0.6}{\epsilon_G}\right)$, which occurs for $L_\lambda \approx 50$, so that $E_{G/F} = E_{G/F}(SNR\uparrow) \sim 2.94$. Thus, for a system with a DISPI length of 50 pixels rather than 180, the grating case outperforms the filter case by a factor of three at all noise levels. Again, because the DISPI over-samples the spectrum by a factor $180/(2R_G)$, a reduction in the resolving power of the grating by a factor 3.6 would be entirely possible.

The results are displayed in figures 2–8. These figures display two $E_{G/F}(V)$ plots (top two panels) and one $SNR^G(V)$ plot (bottom panel). Figure 2 corresponds to the standard WEA2003

case: $N_{obs} = 120; L_\lambda = 180; R_G = 10; R_F = 7, \epsilon_G = 60\%$. For each of the following figures, one parameter has been changed.

Each of these figures contain three panels. The top and middle panels plots the grating efficiency $E_{G/F}(V)$ for the X4 and the X1 binning cases. Each panel shows the results for various noise models, with noise increasing from the top curve to the bottom curve. All figures show the general behavior that $E_{G/F}(V)$ is large for bright stars, and low for faint stars.

The actual SNR values for the grating case are plotted in the bottom panel.

REFERENCES

Bailer-Jones, C. A. L. 2002, Ap&SS, 280, 21

Bailer-Jones, C. A. L. 2000, A&A, 357, 197

Bailer-Jones, C. A. L., Irwin, M., & von Hippel, T. 1998, MNRAS, 298, 361

Cayrel de Strobel G., Soubiran C., Ralite N. 2001, A&AS, 373, 159

Cutri, R. *et al.*, 2003, http://www.ipac.caltech.edu/2mass/releases/allsky/doc/explsup.html

Hauck, B. & Mermilliod, M., 1998, A&AS, 129, 431

Houk, N. & Swift, C., 2000, VizieR Online Data Catalog, 3214

Houk, N. 1971, BAAS, 3, 401

Høg, E. et al. 2000, A&A, 357, 367

Monet, D.G.M, *et al.* 2003, AJ, 125, 984

Olling, 2001, FAME Technical Memorandum #2001-03 http://ad.usno.navy.mil/∼olling/FAME/rpo_fame.htm/ftn

Olling, 2001, FAME Technical Memorandum #2001-07 http://ad.usno.navy.mil/∼olling/FAME/rpo_fame.htm/ftn

Olling, 2001, FAME Technical Memorandum #2001-15 http://ad.usno.navy.mil/∼olling/FAME/rpo_fame.htm/ftn

Soubrian, C., Katz, D. & Cayrel, R., 1998, A&AS, 133, 221

Willemsen, P. G., Bailer-Jones, C. A. L., Kaempf, T. A., & de Boer, K. S. 2003, A&A, 401, 1203

Fig. 1.— The $log(g)$-classification accuracy as a function of photometric error (top panel) and signal-to-noise ratio (bottom panel). Three sets of data are plotted, as well as a fit two of the data sets. The data sets from Olling (2001; triangles) and Wea2003 (stars) do not employ any information bluewards of the Balmer jump, while the Bailer-Jones results (2000, diamonds) were obtained from near-UV and optical data. Fits to the NO-UV results are also indicated. Note that for a given average SNR, the classification results are better when UV data is included.

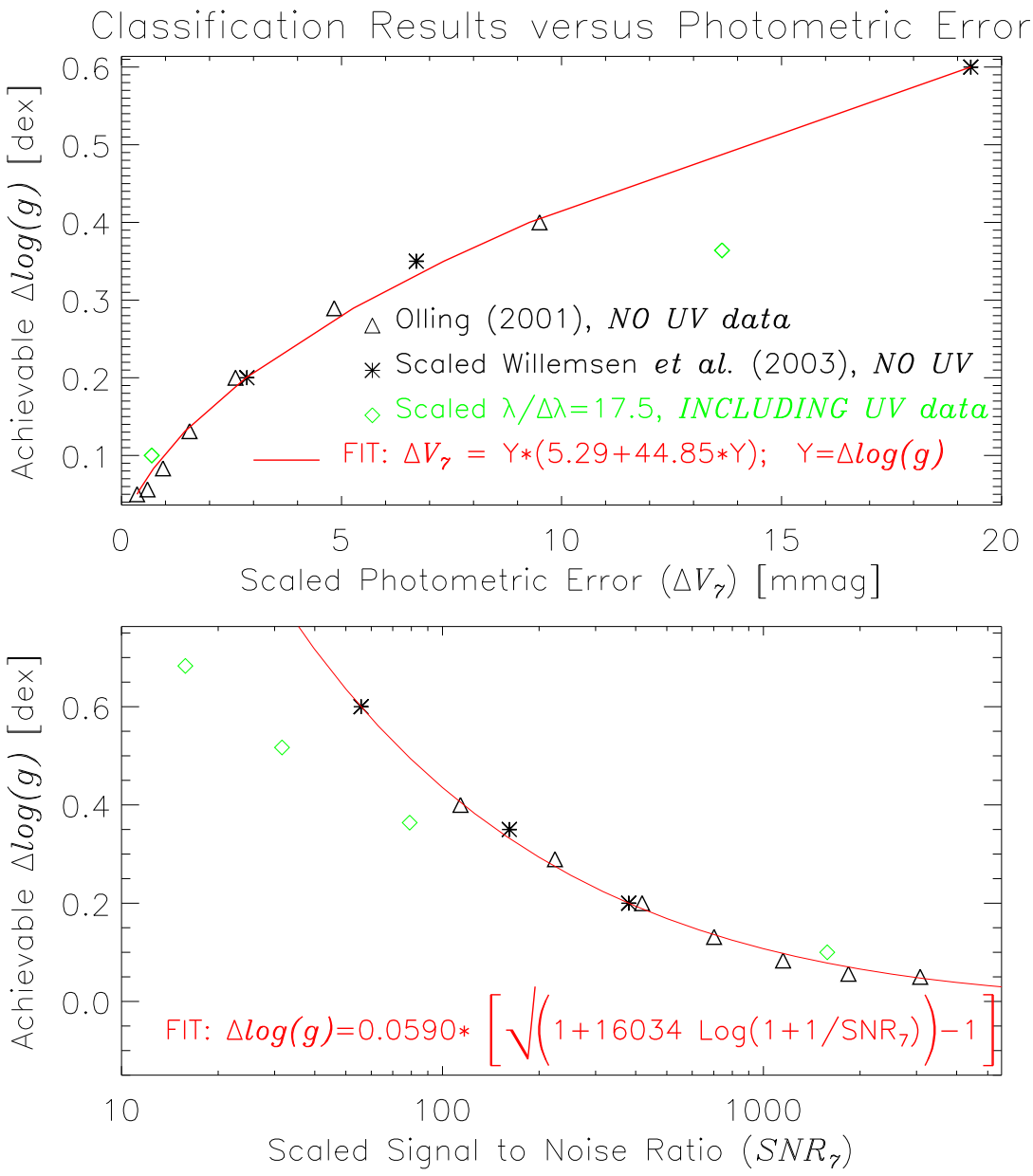

Fig. 2.— The Grating & Filter-Set cases compared. Standard WEA2003 Grating setup & On-chip X4 binning

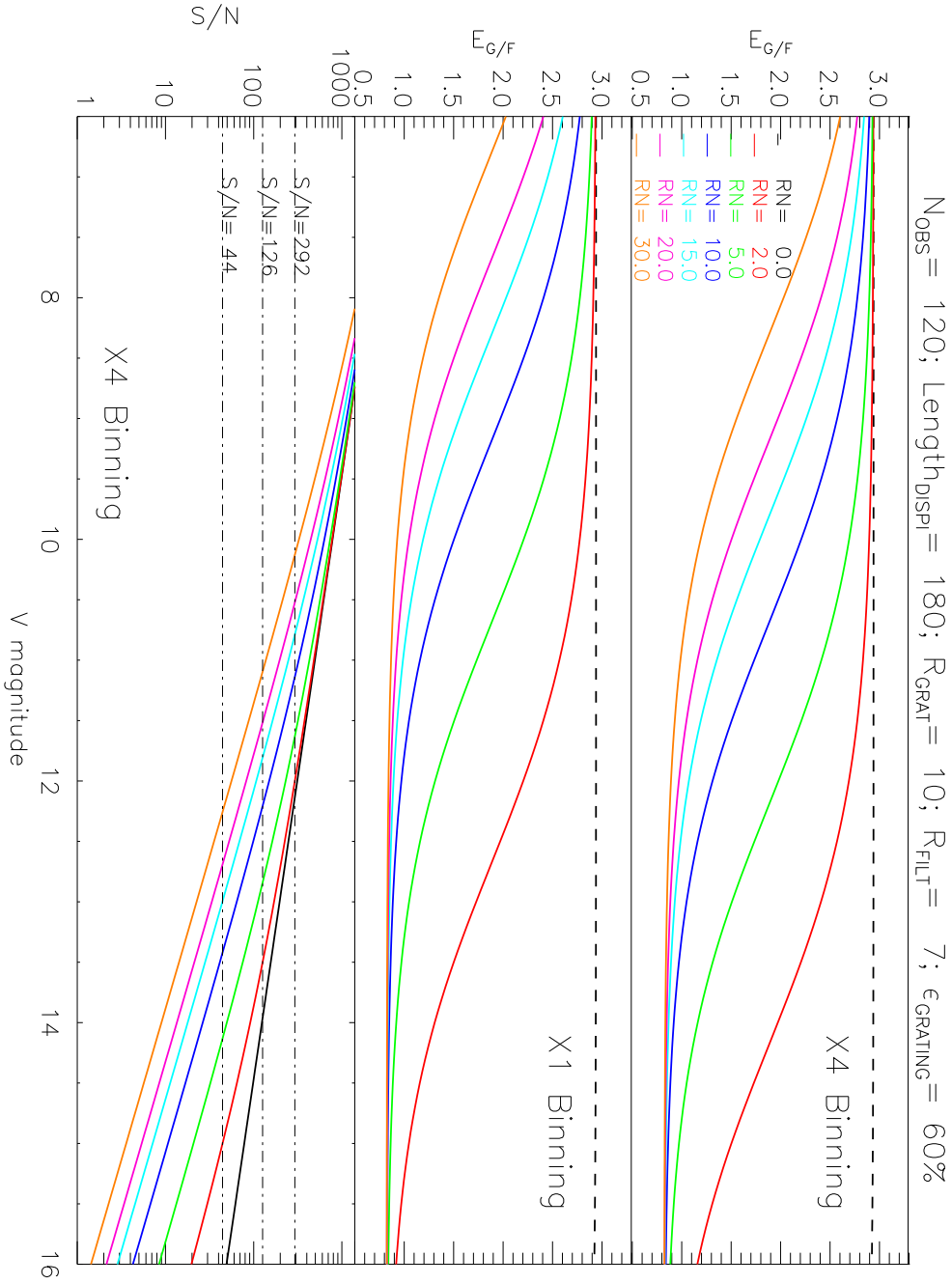

Fig. 3.— The Grating & Filter-Set cases compared. Standard WEA2003 Grating setup & NO on-chip binning

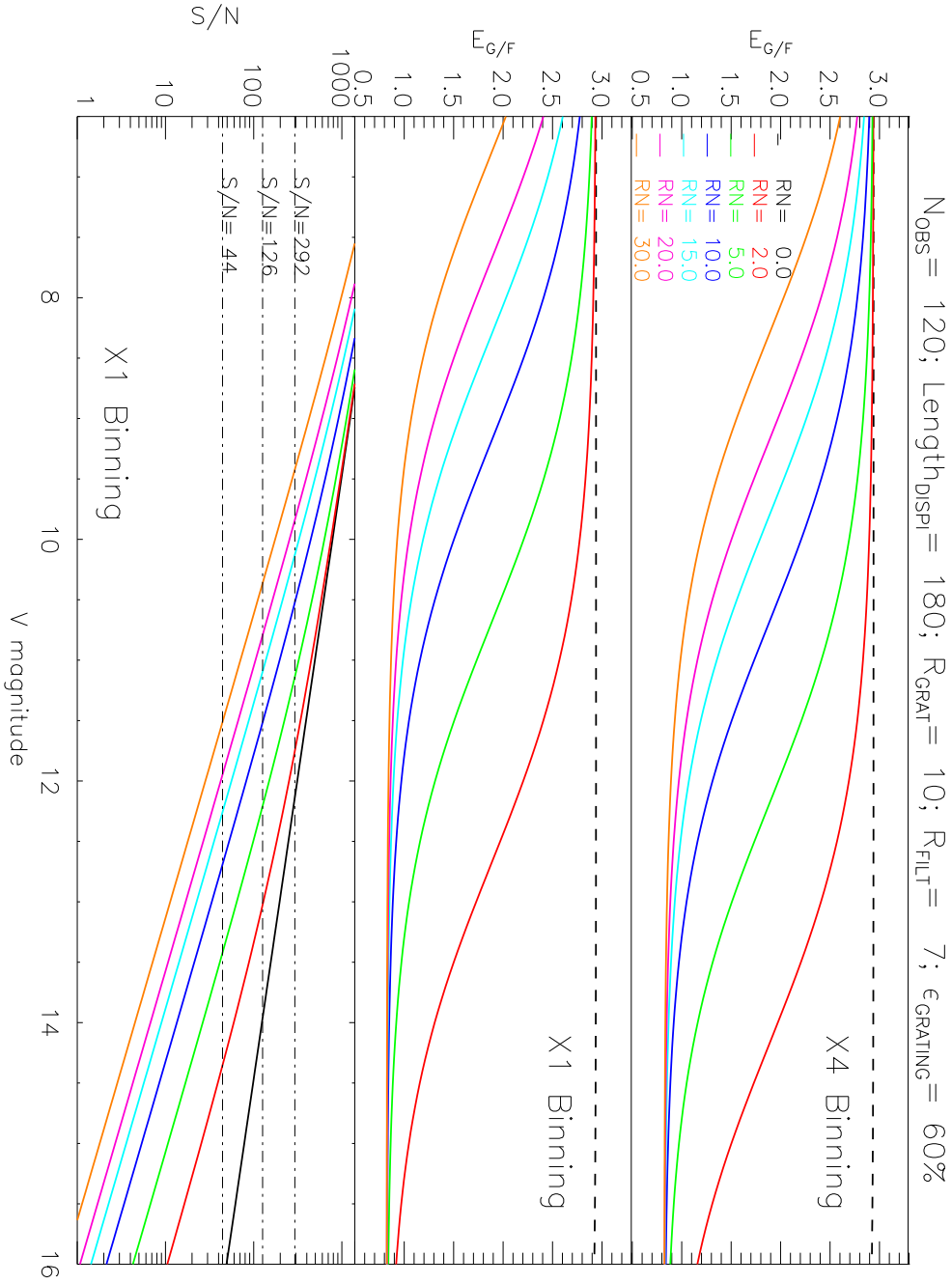

Fig. 4.— The Grating & Filter-Set cases compared. Standard WEA2003 Grating setup & NO on-chip binning & 200 Observations

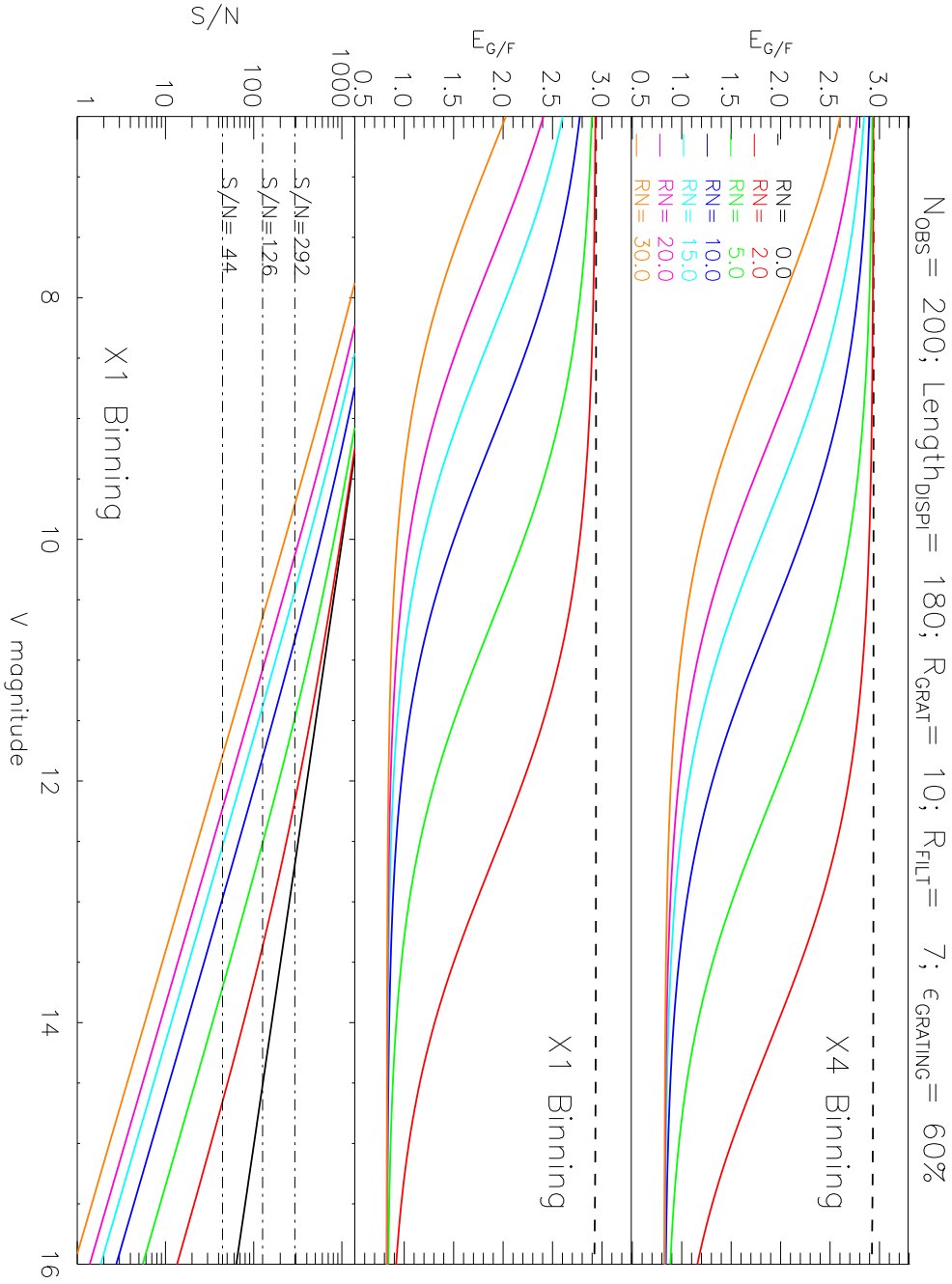

Fig. 5.— The Grating & Filter-Set cases compared. Standard WEA2003 Grating setup & NO on-chip binning & 300 Observations

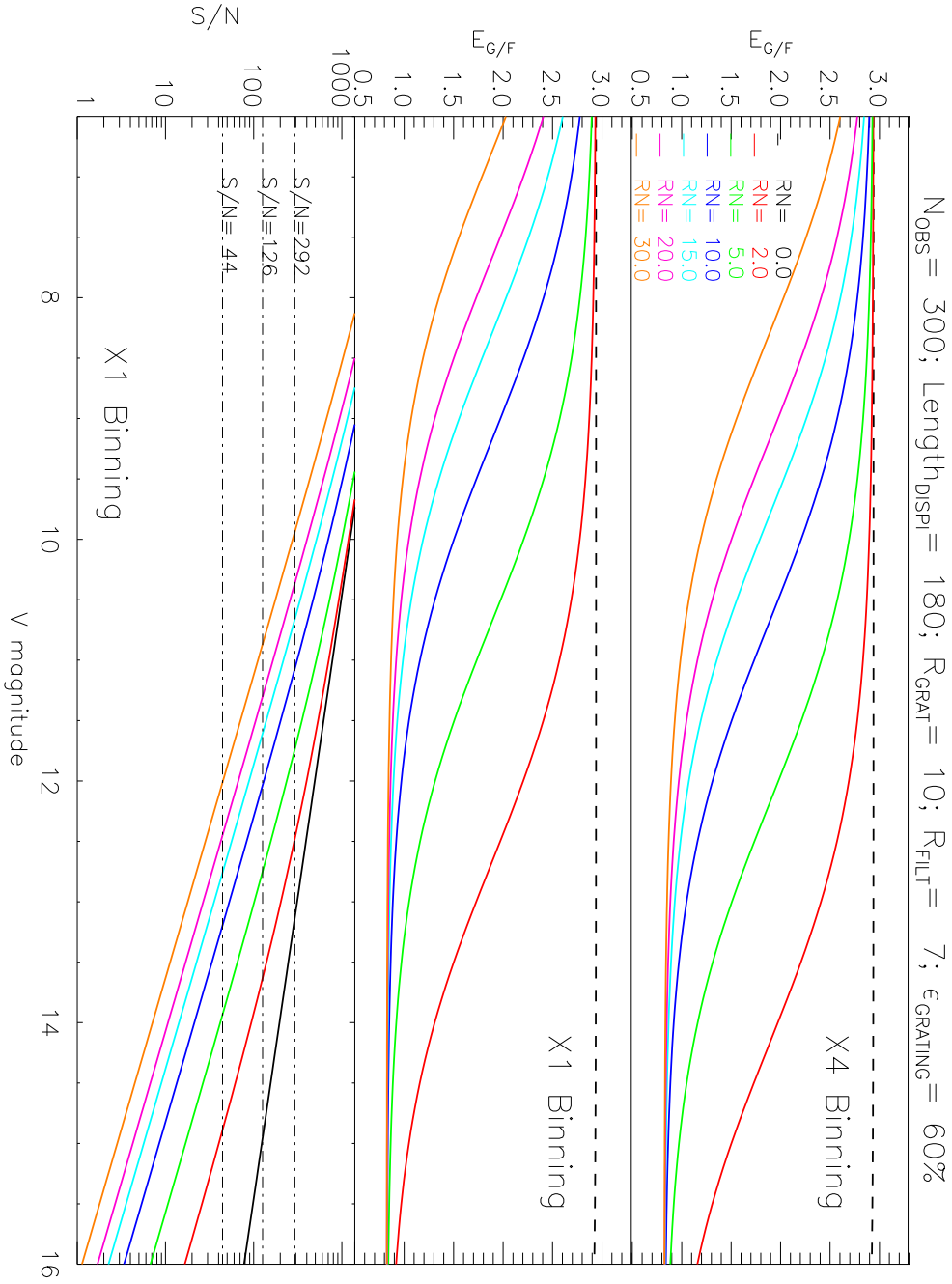

Fig. 6.— The Grating & Filter-Set cases compared. Standard WEA2003 Grating setup & NO on-chip binning & 300 Observations& DISPI length=50 pixels

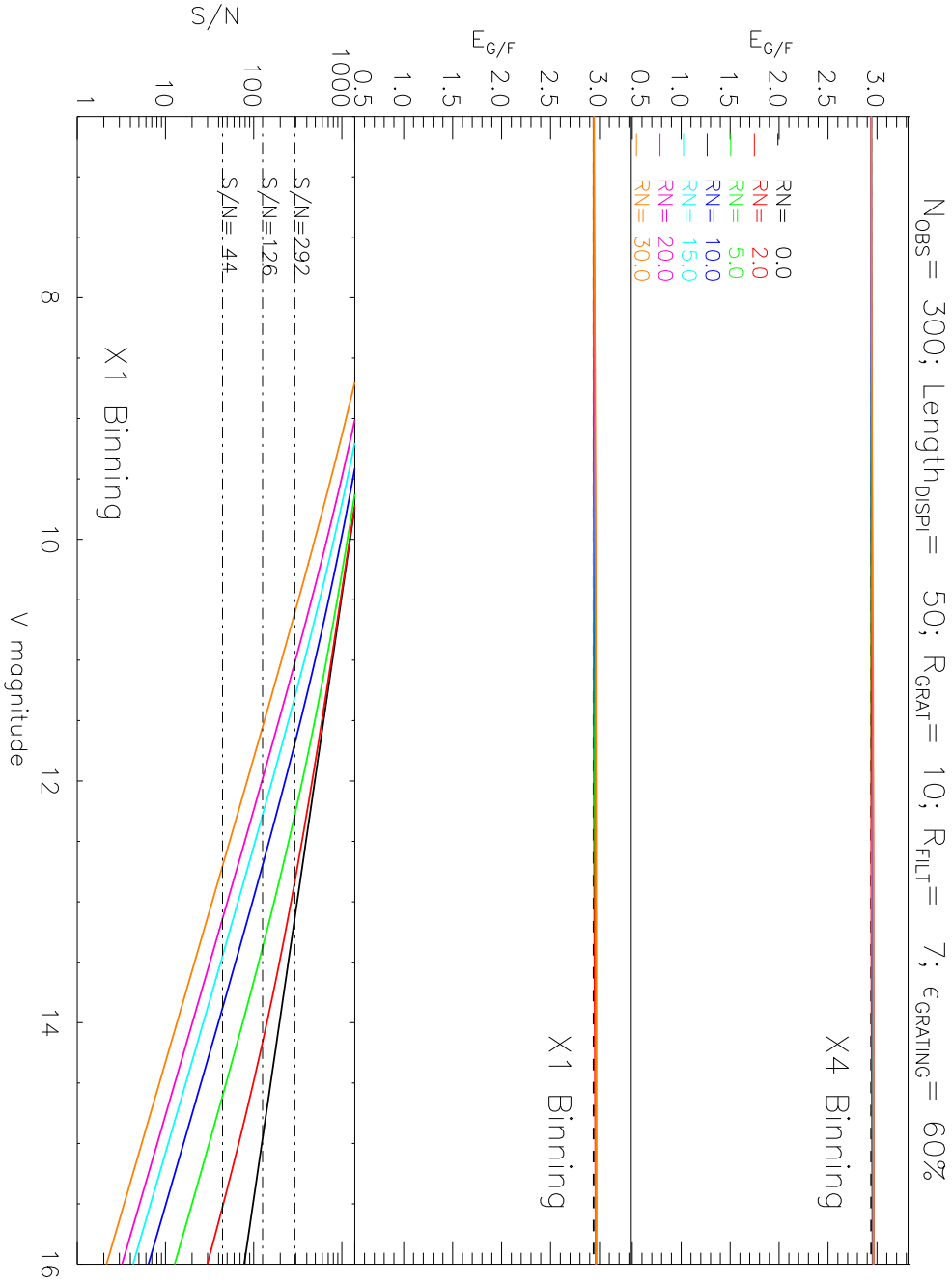

Fig. 7.— The Grating & Filter-Set cases compared. Standard WEA2003 Grating setup & NO on-chip binning & 300 Observations & DISPI length=50 pixels & Grating Efficiency 70%

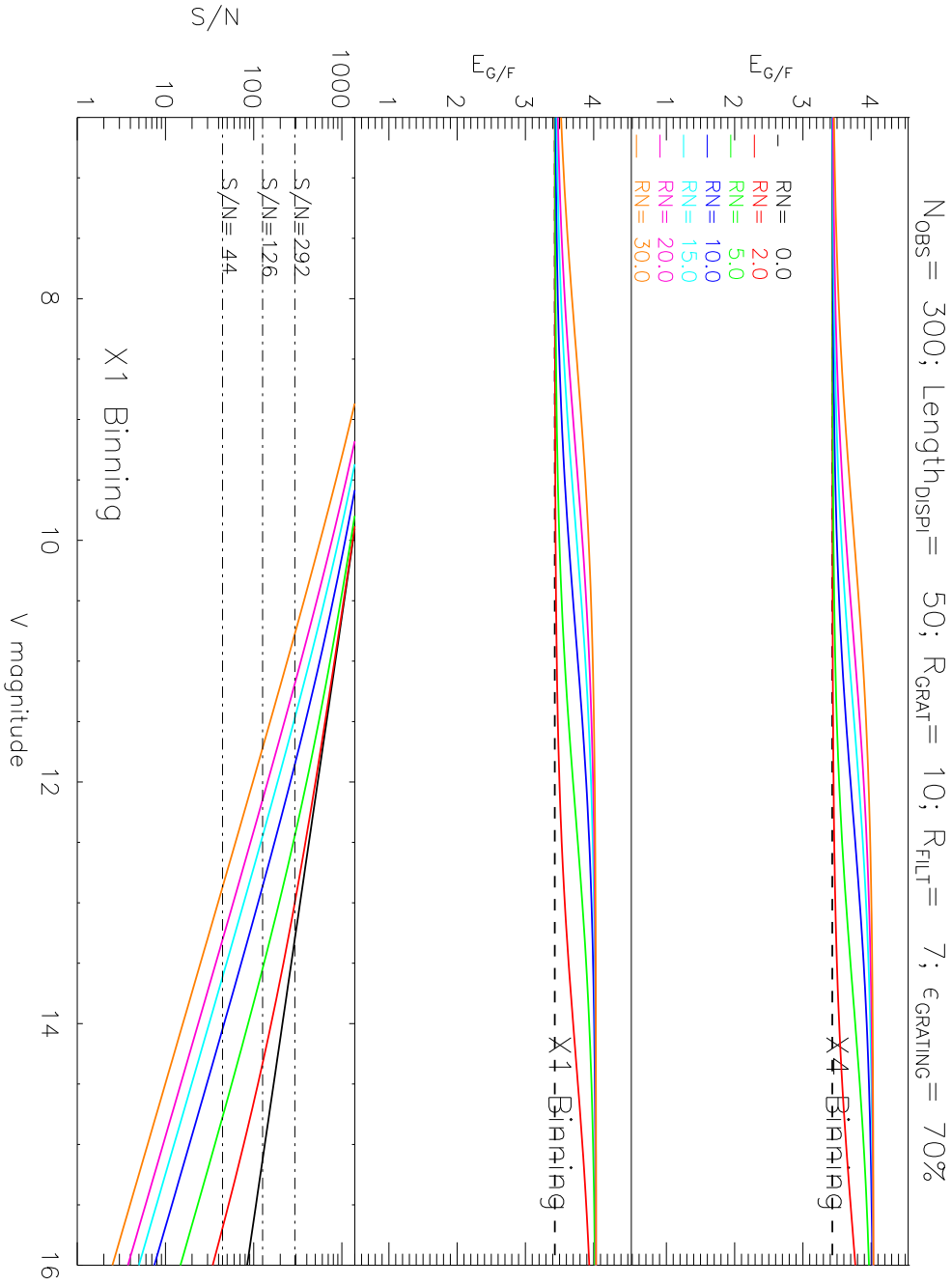

Fig. 8.— The Grating & Filter-Set cases compared. Standard WEA2003 Grating setup & NO on-chip binning & 300 Observations & DISPI length=50 pixels & Grating Efficiency 80%